NEANDC (OR) - 146 "L"
INDC (SWT) - 010 / L

PROGRESS REPORT TO NEANDC FROM SWITZERLAND

June 1976

T. Hürlimann

Swiss Federal Institute for Reactor Research
Würenlingen

~~NOT FOR PUBLICATION~~

PREFACE

This document contains information of a preliminary or private nature and must be used with discretion. Its contents may not be quoted, abstracted, reproduced, transmitted to libraries or societies or formally referred to without the explicit permission of the originator.

CONTENTS

I. Institut de Physique, Université de Neuchâtel

(Dir.: Prof. Jean Rossel)

1. $D(n,n)D$; $D(\vec{n},n)D$ and $D(\vec{n},\vec{n})D$ elastic scattering at low energy

D. Bovet, P. Chatelain, Y. Onel, R. Viennet and J. Weber

The depolarization factor $D(\theta)$ for the scattering of neutrons from deuteron was measured for several angles at 2.45 MeV and the results including some ERA analyses were presented to the 4th International Symposium on Polarization Phenomena, Zürich 1975 {1,2}.

The test of the fast neutron-gamma discriminator {3} has been completed. The performance of this module was of great interest since the discrimination did work up to an average counting rate of 300 KHz, even at low energies.

This module was used in the measurement of the polarization $P(\theta)$ for $\theta_L = 100^o$ at 2.45 MeV which was part of the set of measurements submitted to the International Conference on the Interaction of Neutrons with Nuclei, Lowell Mass., 1976 {4}*). The previous determination of the nd differential cross sections at low energies were not adequate for fitting the data with the available models, even the simplest fit with the orthogonal polynomials was not significant.

Then it has been concluded that there was a need for more accurate differential cross section data, especially at the angles larger than 140^o or 150^o(CM). Therefore we have started to measure the differential cross sections by using the method of recoil energy spectrum {5}.

In this measurement, the scatterer is a NE 213 deuterated liquid scintillator of small dimensions (1 x 1 cm). An associated particle time-of-flight system for the $d(d,n)^3He$ reaction has been developed for producing neutrons of 2.45 MeV. The measurements are in progress.

The measurements of the angular variation of the depolarization factor and other Wolfenstein parameters will be resumed later on.

References

{1} Proceedings of this Conference, contributed papers p. B3

{2} Ibid p. B5

{3} P. Betz et al., Nucl. Instr. & Methods 119 (1974) 199

{4} Proceedings of this Conference, contributed papers (to be published)

{5} D. Bovet, P. Chatelain, Y. Onel, R. Viennet and J. Weber (to be published)

*) This paper also presents some new ERA analyses which include our P(θ) data.

2. Neutron-neutron quasifree scattering at 14.1 MeV

E. Bovet, F. Foroughi, C. Nussbaum and J. Rossel

The differential cross section for the D(n,nn)p reaction has been measured in two different kinematic configurations favouring n-n quasifree scattering where the spectator proton has nearly zero energy. These measurements are a continuation of the preliminary measurements {1} which proved the feasibility of such an experiment without detecting the spectator proton practically at rest in the C_6D_{12} target. The two symmetrical configurations, $\theta_1=\theta_2=40^o$, $\theta_{12}=180^o$ ($E_p^{min}=0$) and $\theta_1=\theta_2=30^o$ ($E_p^{min}=180$ keV), were chosen to favour comparison with existing "exact" theoretical predictions, for which such configurations are particularly well suited {2}. The electronic signals directly related to the deuteron break-up, as well as those controlling the stability of the experiment were processed and stored by a PDP 15/20 computer. In addition, the simultaneous measurements of the yields from the D(n,n)D and $^{12}C(n,n)^{12}C$ elastic reactions which are used to monitor the break-up reaction, were also recorded by the computer.

The data analysis shows:

a) that such an experiment can be successfully performed without detecting the spectator proton ($\sim 2 \cdot 10^3$ true events for $2{,}2 \cdot 10^3$ counts in 2000 hours);

b) that the differential cross section at $\theta_1 = \theta_2 = 40^\circ$ ($E_p = 0$) is smaller than that of $\theta_1 = \theta_2 = 30^\circ$ by a factor of about 2, whereas the "exact" {3} theory (Faddeev equations with separable two-body potentials) predicts a factor of only 1.3;

c) that the shape of the differential cross section obtained at 30° shows evidence of a pronounced relative minimum for $E_p = E_p^{min} = 180$ keV. This structure is predicted by neither the simpler {4} nor the more sophisticated "exact" theoretical models using s-wave nucleon-nucleon interaction.

References

{1} E. Bovet, F. Foroughi and J. Rossel, Helv. Phys. Acta 48 (1975) 137

{2} M. Jain, J. G. Rogers and D. P. Saylor, Phys. Rev. Lett. 31 (1973) 838

{3} W. Ebenhöh, Nucl. Phys. A191 (1972) 97

{4} F. Foroughi and E. Bovet, Helv. Phys. Acta 48 (1975), 577

II. Laboratorium für Kernphysik, Eidg. Technische Hochschule Zürich

(Dir.: Prof. Dr. J. Lang)

1. Measurement of the analysing powers in $^3He(\vec{d},d)^3He$ Scattering

B. Jenny, W. Grüebler, V. König, P. A. Schmelzbach, R. Risler, D. O. Boerma and W. G. Weitkamp

Some time ago, a phase shift analysis based on the cross section and all analysing power components of d-^{3}He elastic scattering has been tried. Measurements of iT_{11}, T_{20}, T_{21} and T_{22} exist in the energy range between 4.0 and 11.5 MeV {1}. Due to the relatively complicated spin structure of the scattering problem and the existence of open reaction channels, the scattering matrix contains a large number of independent elements. In fact, the phase shift analysis showed clearly the need for extended and more precise data in order to determine the matrix elements accurately. Measurements in smaller energy steps and at lower energies were also desirable.

New angular distributions of iT_{11}, T_{20}, T_{21}, T_{22}, and of the unpolarized differential cross section have been measured for ten deuteron bombarding energies between 2.0 and 11.5 MeV, each containing up to 50 data points with a relative error in the analysing powers of typically 0.005. It was possible to extend the measurements to c. m. angles of 12.5^o and 165^o using a special gas target with 0.9 mg/cm^2 mylar foil entrance and exit windows. The ^{3}He gas pressure was 200 Torr. The beam polarization was determined with a polarimeter mounted behind the target.

Fig. 1 shows two of the measured analysing powers. Circles indicate data points obtained by detecting the recoil ^{3}He particles. A comparison with measurements of $^3H(\vec{d},d)^3H$ scattering {2} at the same deuteron energies is interesting. Generally they agree remarkably well with $^3He(\vec{d},d)^3He$ scattering, thus confirming the similarity of ^{5}He and its mirror nucleus at higher excitation energies, where a series of T = 1/2 levels is predicted by theoretical calculations {3,4,5}. One part of the occuring significant deviations

may probably be ascribed to the 0.24 MeV higher excitation of the ^{5}He nucleus resulting from the different threshold energies. The discrepancies of T_{22} at 5.0 MeV between 30^o and 60^o and those at 8.0 MeV seem to be caused by other reasons. A phase shift analysis of the new data is now in progress at this laboratory.

References

{1} V. König, W. Grüebler, R. E. White, P. A. Schmelzbach and P. Marmier, Nucl. Phys. A185 (1972) 263

{2} A. A. Debenham, V. König, W. Grüebler, P. A. Schmelzbach, R. Risler and D. O. Boerma, Nucl. Phys. A216 (1973) 42

{3} P. Heiss and H. H. Hackenbroich, Nucl. Phys. A162 (1971) 530

{4} R. F. Wagner and C. Werntz, Phys. Rev. C4 (1971) 1

{5} F. S. Chwieroth, R. E. Brown, Y. C. Tang and D. R. Thompson, Phys. Rev. C8 (1973) 938

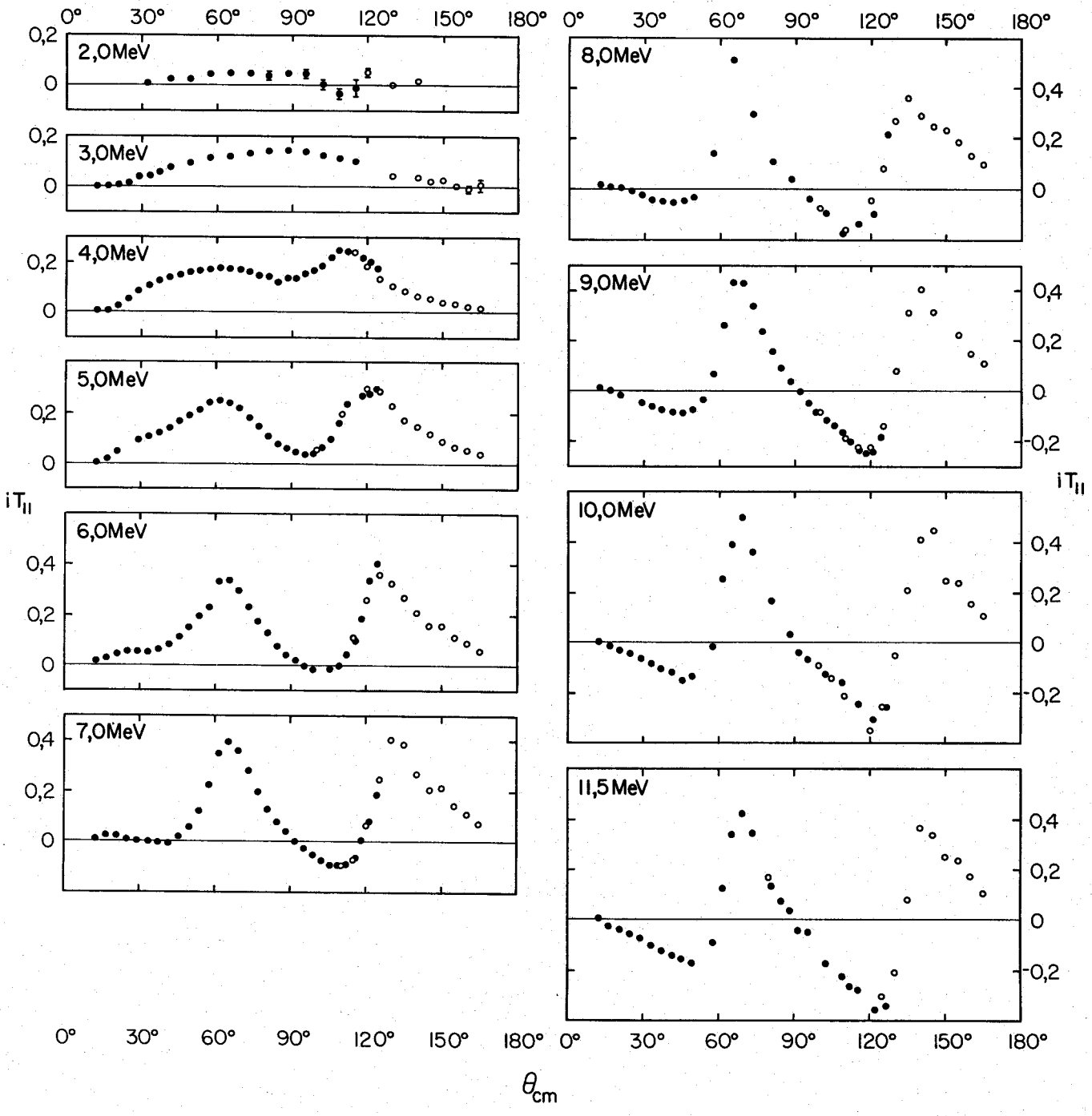

Fig. 1: Vector analysing power iT_{11} in $^{3}He(\vec{d},d)^{3}He$ scattering

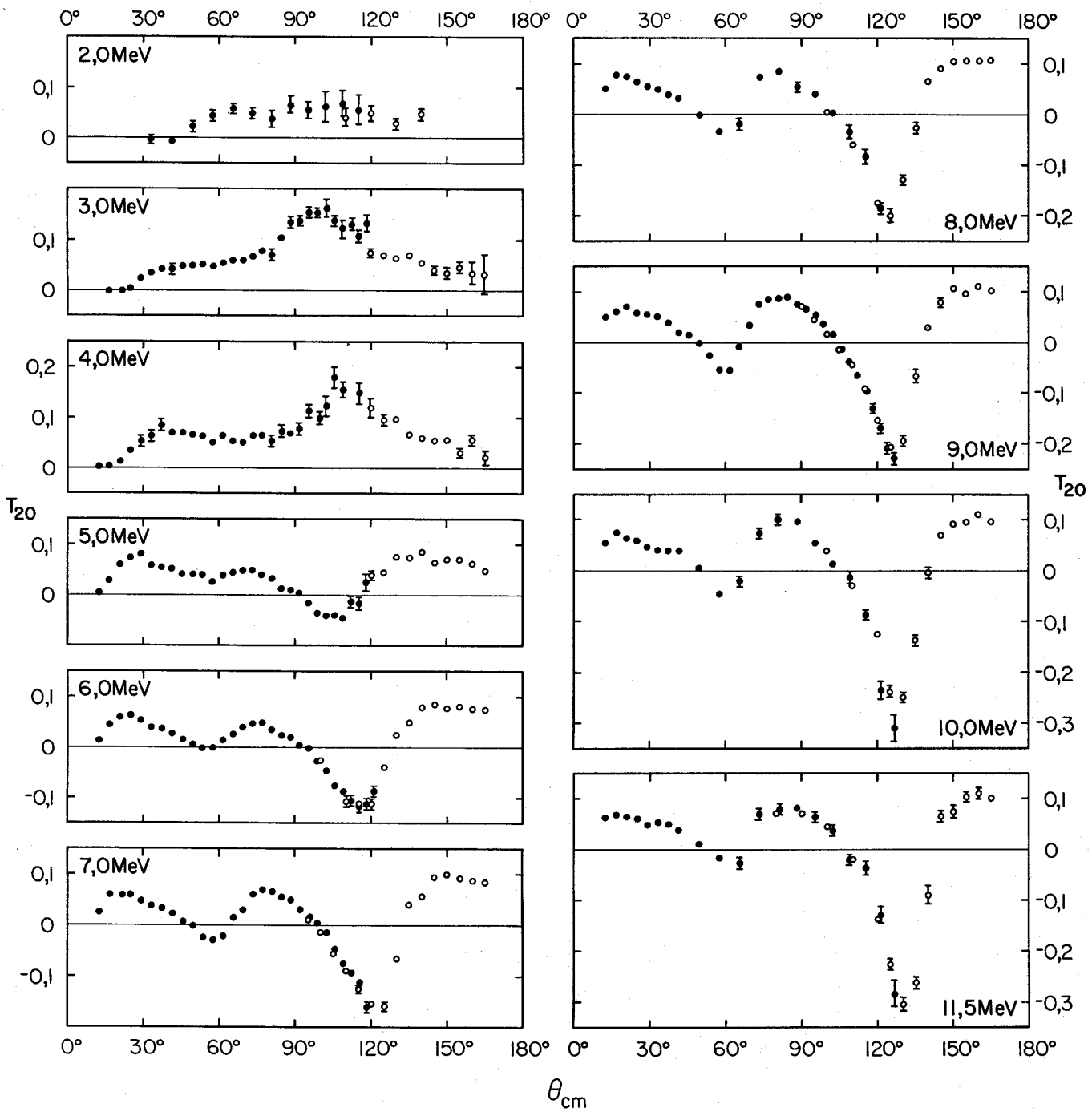

Fig. 2: Tensor analysing power T_{20} in $^{3}He(\vec{d},d)^{3}He$ scattering

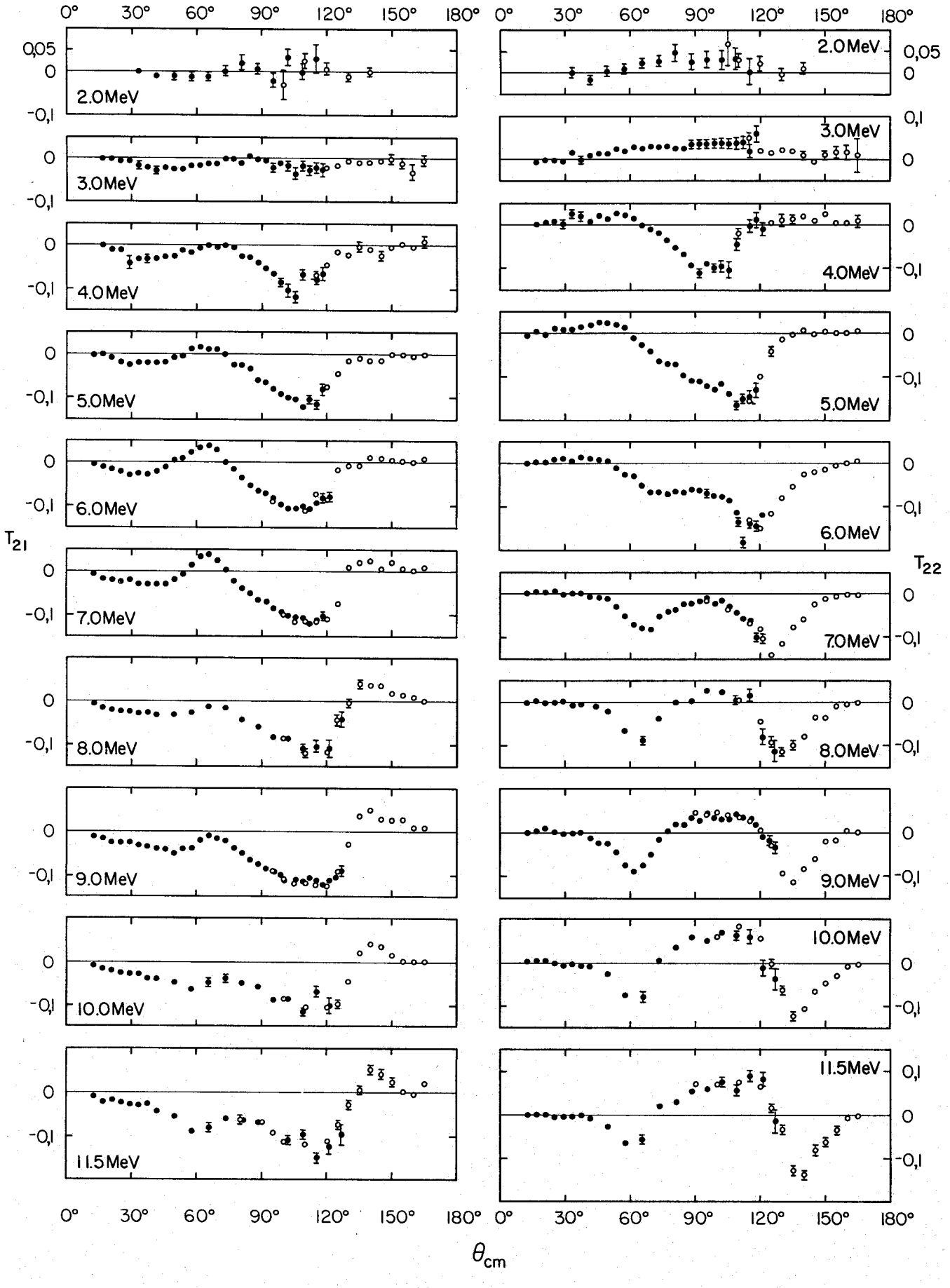

Fig. 3: Tensor analysing powers T_{21} and T_{22} in $^{3}He(\vec{d},d)^{3}He$ scattering

2. Elastic Scattering of ^{9}Be Ions

J. Lang, R. Müller, E. Ungricht and J. Unternährer
L. Jarczyk†, A. Strzalkowski† and R. Bukowska†

The angular distribution for elastic scattering of ^{9}Be ions on different nuclei were measured using the ^{9}Be beam from the ETH tandem accelerator in Zürich {1}. The measurements were performed for the target nuclei ^{9}Be, ^{12}C, ^{24}Mg, ^{27}Al, ^{28}Si, ^{40}Ca, ^{58}Ni and ^{108}Ag at the three beam energies 14, 20 and 26 MeV. The angular region from 10^{o} to 100^{o} (Lab) and in some cases up to 160^{o} was covered in 5^{o} intervals.

Except for the lightest investigated nuclei ^{9}Be and ^{12}C where some structure in the angular distributions was observed, only a smooth decrease of the cross section above some angle could be noticed, characteristic for the strong absorption and domination of Coulomb interaction. Following a procedure used in {2}, experimental results at 20 MeV are presented in Fig. 1 in function of $d=D(\theta)/(A_1^{1/3}+A_2^{1/3})$, where $D(\theta)$ is the distance of closest approach corresponding to the classical Coulomb orbit. This representation

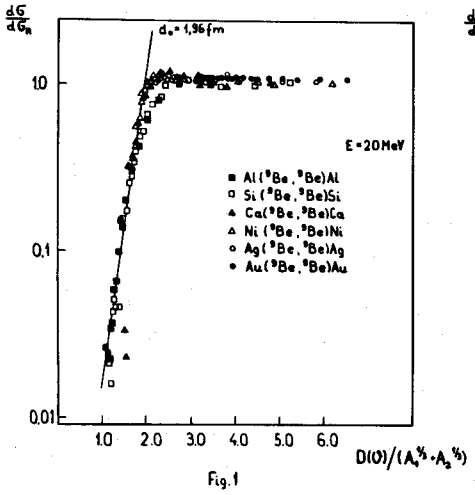

Fig.1

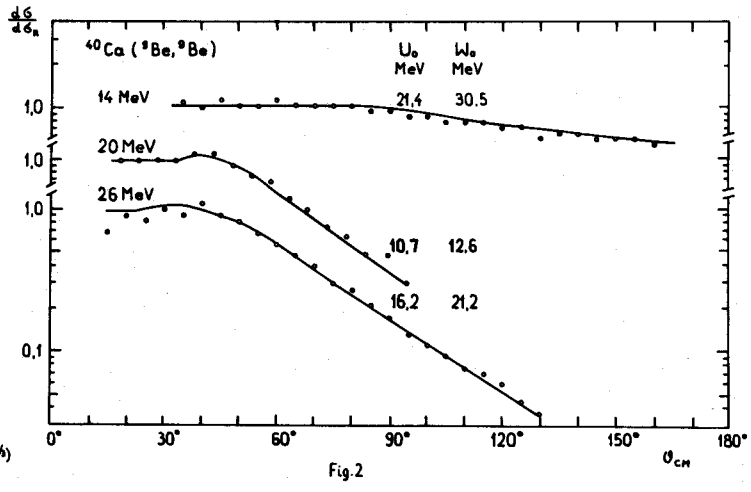

Fig.2

shows that the distance D_o for which nuclear effects set in varies proportional to $(A_1^{1/3}+A_2^{1/3})$ resulting in an approximately constant d_o of 1.96 fm. This value is, however, greater than the distances found in ^{16}O or ^{12}C scattering. The optical model can, of course, be used to fit the cross sections.

It is well known that the optical model parameters cannot be determined in an unique way from such measurements. Therefore, the geometrical parameters were fixed arbitrarily to $R=1{,}27\ (A_1^{1/3}+A_2^{1/3})$ fm and $a=0{,}647$ fm and only the depths of the real and imaginary potentials varied. An example is given in Fig. 2.

References

{1} R. Balzer, contribution to Heavy Ion Conference, Caen, September 1976

{2} G. R. Satchler, Reaction between Complex Nuclei, Tennessee 1974

† Institute of Physics, Jagellonian University, 30059 Cracow, Poland

III. Institut für Physik der Universität Basel

(Dir.: Prof. E. Baumgartner)

Spectroscopic Factors for Energy Levels of $^{41,43,45,49}Ca$

H. Schär, D. Trautmann and E. Baumgartner

In this work we briefly describe the determination of spectroscopic factors by means of (d,p) reactions on some Calcium isotopes in the vicinity of the Coulomb barrier.

Differential (d,p) cross-sections on $^{40,42,44,48}Ca$ were measured at 2.5 MeV incident deuteron energy in 5 degree intervals between 40 and 160 degrees. The excitation energies of the final nuclei range from 0 to 5.5 MeV.

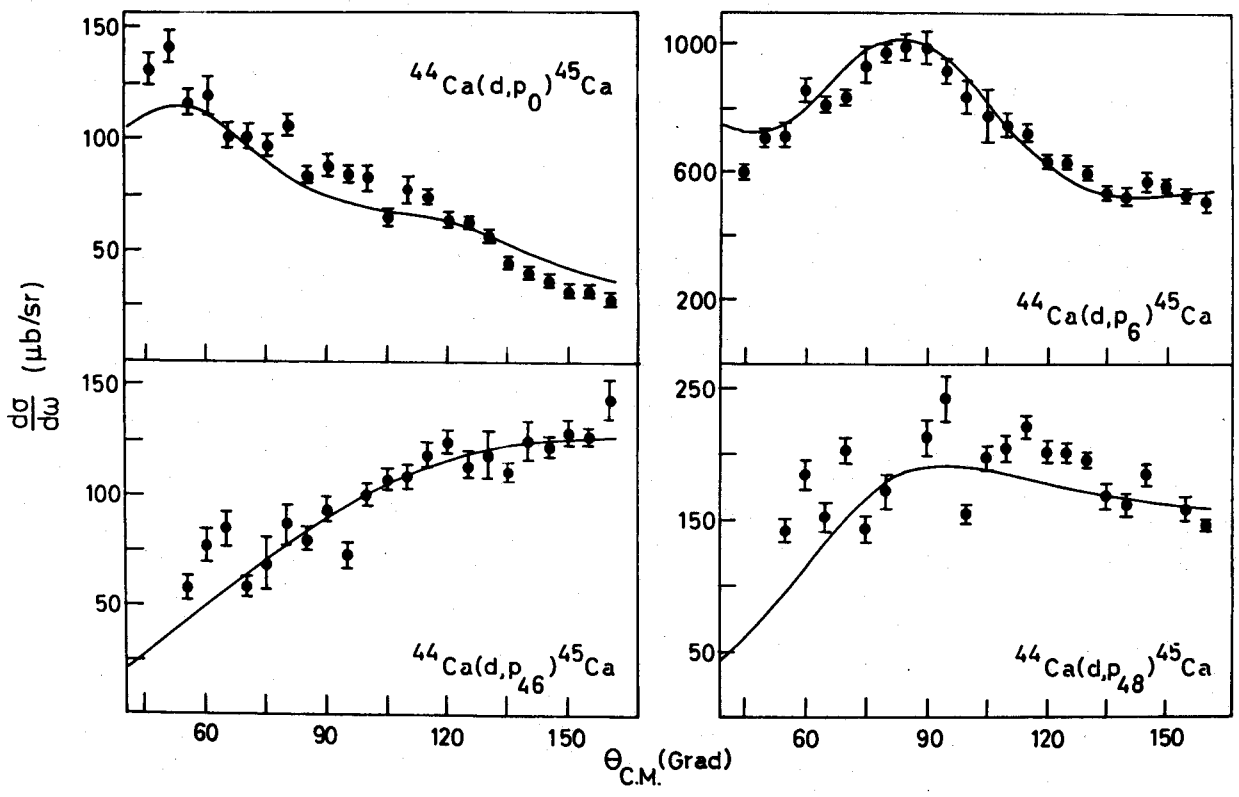

Fig. 1: Measured and calculated angular distributions of the reactions $^{44}Ca(d,p)^{45}Ca$ at 2.5 MeV deuteron energy. The corresponding level energies and spectroscopic factors are summarized in table 1. The quantity j is the total angular momentum.

Theoretical angular distributions are calculated with the Born approximation. However, as usual the plane waves are replaced by waves calculated in an optical model potential, using the computer codes DWUCK {1} and LOLA {2}. A least squares' fit of these angular distributions to the measured cross-sections gives the spectroscopic factors.

Fig. 1 shows selected angular distributions; the dots are the experimental values, the full lines represent the results obtained with the code DWUCK.

Table 1: Spectroscopic Information for ^{45}Ca

level No.	excitation energy (MeV)	ℓ	2j	(2j+1)S
0	0.000	3	7	3.6
6	1.904	1	3	2.5
46	4.837	2	5	0.5
48	4.919	0	1	0.1

When the energies of the incoming deuteron and the outgoing proton are both well below the Coulomb barrier, the spectroscopic factor is almost independent of the optical scattering potentials; it is only influenced by the optical model parameters describing the bound neutron wave-function.

Unfortunately, pure subcoulomb conditions cannot be realized for every energy level in the final nucleus because of the high reaction Q values {3}. Possible compound nuclear contributions to the cross-section, and ambiguities in the choice of the optical model parameters render an exact determination of spectroscopic factors difficult.

References

{1} P. D. Kunz, University of Colorado, Internal Report COO-535-613

{2} R. M. de Vries, Phys. Rev. C8, 951 (1973)

{3} F. K. Mc Gowan and W. T. Milner, Nucl. Data Tables 11, 1 (1972)

IV. Physik-Institut der Universität Zürich

(Dir.: Prof. E. Brun)

^{3}He Induced Activation Cross Sections on ^{10}B, ^{16}O and ^{19}F

J. Gass and H. H. Müller

With respect to the interpretation of activation analyses, activation cross sections for the reactions $^{10}B(^{3}He,d)^{11}C$, $^{16}O(^{3}He,p)^{18}F$ and $^{19}F(^{3}He,\alpha)^{18}F$ have been determined in the energy range of the incident particle between 1.5 and 4.6 MeV. The production yield of activated nuclei in a thick target was measured as a function of the incident particle energy. The cross section values have been determined by differentation of the yield curves.

In Fig. 1 are shown the activation cross sections obtained in the present measurements along with those of Hahn at al {1} for the reactions $^{16}O(^{3}He,p)^{18}F$ and $^{19}F(^{3}He,\alpha)^{18}F$ and of Patterson et al {2} for the reaction $^{10}B(^{3}He,d)^{11}C$. A summary of the numerical data is given in Table 1.

A more detailed article to this subjet will be published in Nuclear Instruments and Methods.

References

{1} R. L. Hahn and E. Ricci
Physical Review 46 (1966) 650

{2} J. P. Patterson, J. M. Poate, E. W. Titterton and B. A. Robson
Proc. Phys. Soc. 86 (1965) 1297

Table 1: Numerical values of the activation cross sections $\sigma(E_o)$ (in mb)

Energy interval (MeV)	$^{16}O(^{3}He,p)^{18}F$	$^{19}F(^{3}He,\alpha)^{18}F$	$^{10}B(^{3}He,d)^{11}C$
1,2 -1,4			0,31 ± 0,02
1,4 -1,6			1,08 ± 0,07
1,5 -1,75	0,71 ± 0,01		
1,6 -1,8	0,76 ± 0,02		2,40 ± 0,20
1,75 2,0	1,93 ± 0,04		
1,8 -2,0	1,82 ± 0,09		5,17 ± 0,45
2,0 -2,125	3,85 ± 0,12		
2,0 -2,2	3,61 ± 0,21		8,7 ± 0,9
2,0 -2,5		0,33 ± 0,10	
2,125-2,25	7,05 ± 0,22		
2,2 -2,4	11,2 ± 0,6		5,7 ± 1,3
2,25 -2,375	16,9 ± 0,5		
2,25 -2,5		0,82 ± 0,03	
2,375-2,5	23,3 ± 0,7		
2,4 -2,5	21,0 ± 1,9		30,6 ± 4,1
2,5 -2,6	19,1 ± 2,7		29,0 ± 6,1
2,5 -2,625	14,4 ± 0,9	3,9 ± 0,2	
2,6 -2,8	27,3 ± 2,1		14,9 ± 3,9
2,625-2,75	21,9 ± 1,1	4,5 ± 0,3	
2,75 -2,875	31,1 ± 1,6	6,9 ± 0,5	
2,8 -3,0	43,3 ± 3,5		33,4 ± 5,5
2,875-3,0	59,3 ± 2,4	4,3 ± 0,6	
3,0 -3,125	50,7 ± 2,9	5,0 ± 0,7	
3,0 -3,2	70,7 ± 5,8		26,1 ± 7,0
3,125-3,25	62,2 ± 3,7	16,8 ± 1,0	
3,2 -3,4	95,1 ± 9,0		22,4 ± 8,5
3,25 -3,375	53,9 ± 4,4	6,9 ± 1,2	
3,375-3,5		9,0 ± 1,5	
3,4 -3,6	86 ± 12		28 ± 10
3,5 -3,625		18,4 ± 1,8	
3,6 -3,8	108 ± 16		15 ± 11
3,8 -4,0	129 ± 20		17 ± 12
4,0 -4,2	171 ± 26		63 ± 14
4,2 -4,4	205 ± 33		47 ± 17
4,4 -4,6	139 ± 39		75 ± 21

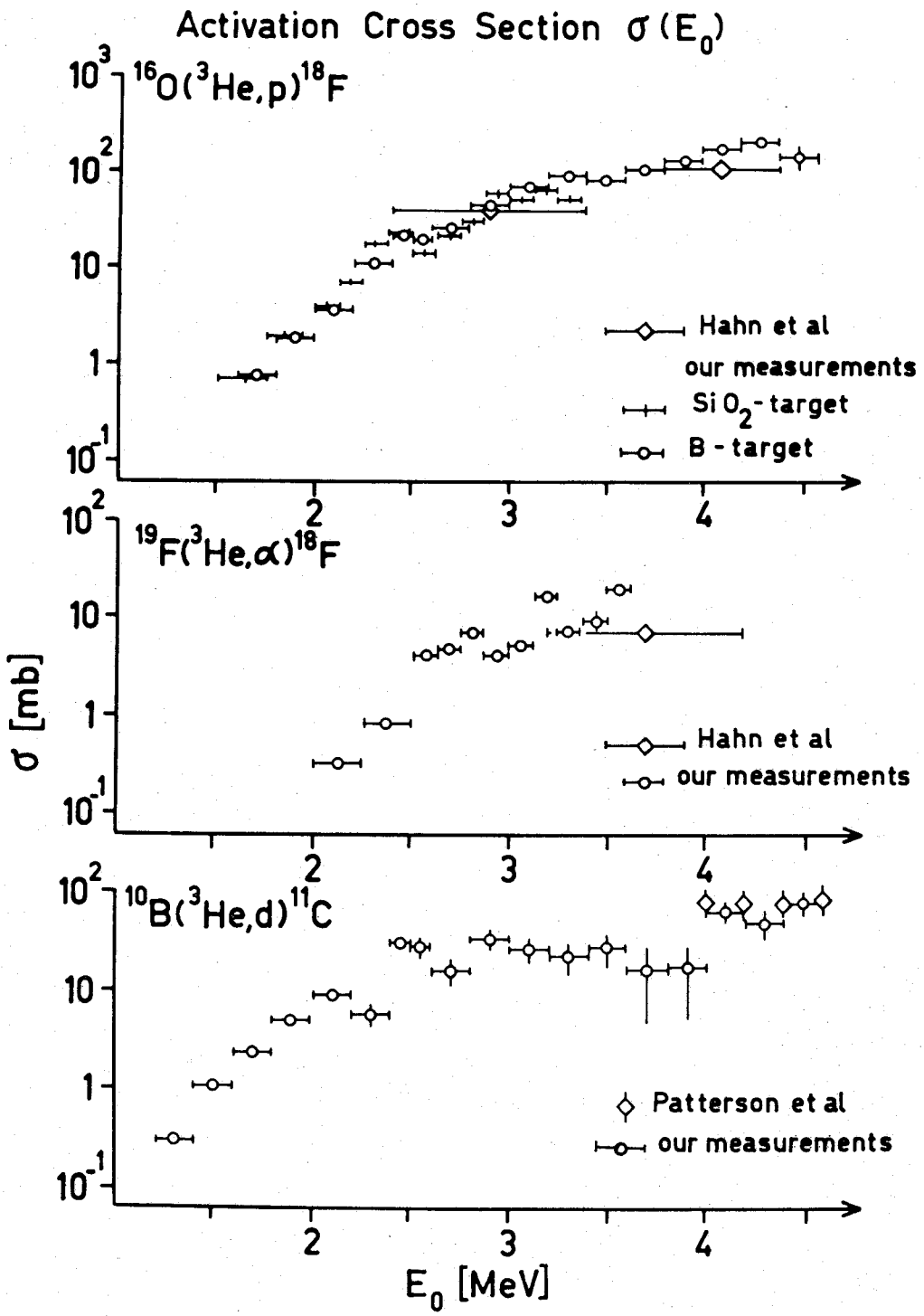

Fig. 1: Activation cross sections as functions of energy. As target material for the reaction $^{16}O(^{3}He,p)^{18}F$ we used clean quartz glass (SiO_2), CaF_2-powder pressed to tablets for the reaction $^{19}F(^{3}He,\alpha)^{18}F$ and tablets of natural boron-powder for the reaction $^{10}B(^{3}He,d)^{11}C$. Relative oxygen cross section values could also be extracted from the boron measurements, as the boron-powder was partially oxidized.

V. Eidg. Institut für Reaktorforschung, Würenlingen

(Dir.: Prof. H. Gränicher)

1. Dynamic Fission Barriers of Even-Even Actinides Nuclei

K. Junker

Based on the concept of dynamic fission paths (1) the fission barrier of about 60 nuclei in the range from Th to Ku have been calculated. Using a realistic shell model potential (deformed Woods-Saxon potential including the Coulomb potential for the protons {2,3}) to generate the single particle states, the potential energy surfaces of the actinide nuclei have been determined by applying Strutinskys' energy renormalization method {4}. The shape parametrization of H. C. Pauli {5} has been used and supplemented by a further deformation parameter describing deviations from axial symmetry. The calculation included elongation, constriction and axial asymmetry at the inner barrier and elongation, constriction and mass asymmetry at the outer barrier. Fig. 1 shows the calculated barriers as a function of Z^2/A of the fissioning nuclei. The values are given with respect to the groundstate and include 0,5 MeV zero point energy. In Fig. 2 the expected mass asymmetry χ (ratio of the volume of the heavy fragment to that of the light fragment) determined at the outer dynamic barrier is shown as a function of the mass number A. Preliminary investigations for the Pu isotopes showed a remarkable instability of the outer, mass symmetric barrier against axially asymmetric distortions. As much as 2 MeV barrier reduction is obtained by including axial asymmetry in the calculations. As a consequence the difference ΔE_B between mass symmetric and mass asymmetric outer barriers was calculated to be approximately 1,5 MeV independent of the neutron number N. This fits nicely to the experimental results {6} which never showed the pronounced maximum of about 4 MeV at a neutron number $N \simeq 146$ predicted by all previous calculations.

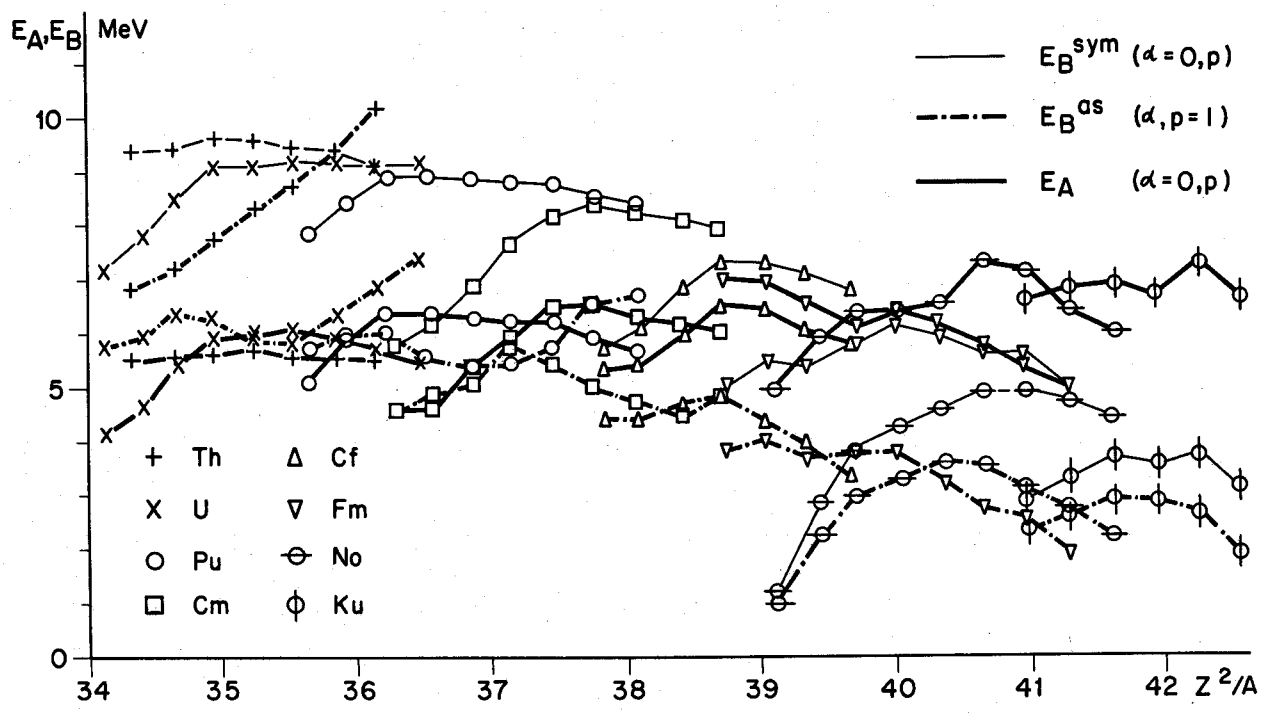

Fig. 1: Fission barriers as a function of Z^2/A (E_A: inner barrier, E_B: outer barrier). Values are given with respect to the groundstate energy, including 0.5 MeV zero point energy.

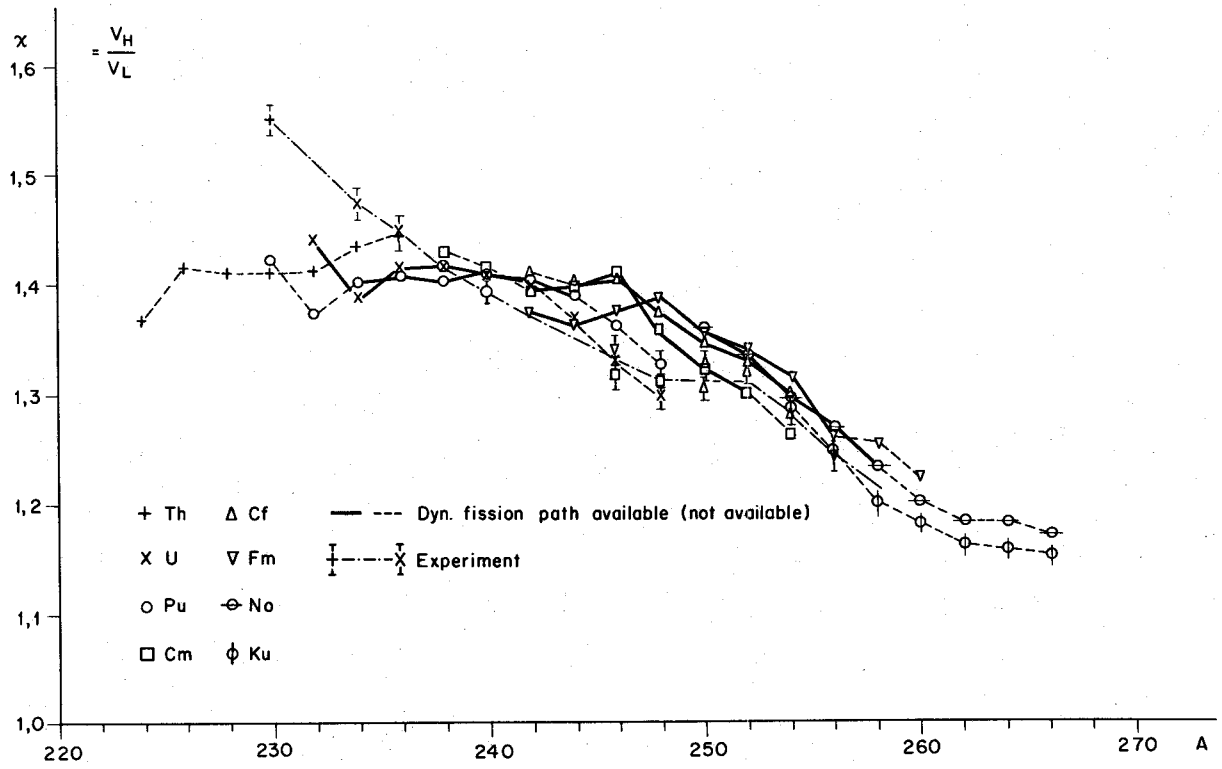

Fig. 2: Mass asymmetry determined at the outer dynamic fission barrier

References

{1} T. Ledergerber and H. C. Pauli, Nucl. Phys. A207 (1973), 1

{2} K. Junker, Acta Phys. Austr. 40 (1974), 335

{3} K. Junker, Acta Phys. Austr. 43 (1975), 221

{4} V. M. Strutinsky, Nucl. Phys. A122 (1968), 1

{5} H. C. Pauli, Phys. Rep. 7C (1972)

{6} H. J. Specht, Proc. Seventh Masurian School in Nucl. Phys., Part3, Nukleonika 20 (1975), 717

2. Production of Radioisotopes with 500 MeV Protons

J. Hadermann

The feasibility of ^{123}I production by 500 MeV protons from different target nuclei is investigated. Cross sections for spallation and peripheral reactions are calculated in the framework of a parametric representation {1}. Table 1 gives a comparison of available experimental and calculated cross sections in the mass and energy region of interest. Cumulative cross sections are indicated by curly brackets. Generally calculated and experimental values agree reasonably well. It would, however, be useful to fill some of the experimental gaps and to check some of the larger discrepancies.

In table 2 cumulative activities for different Xenon isotopes* were calculated taking into account the radioactive decay chains of the isotopes produced. For the beam and target specifications shown in the table caption activities between 650 mCi and 2Ci were obtained. The ratio R: = ^{123}Xe activity / ^{121}Xe activity is important in minimizing the most unwanted ^{121}I contamination. The isotopes ^{134}Ba and ^{135}Ba would be the most suitable targets for ^{123}I production. However, as a readily available target material ^{133}Cs is competing favorably.

* For the production of ^{123}I Xenon is blown out from the irradiated target enhancing the purity of the desired iodine isotope.

Table 1a

Product	^{139}La - Target			^{123}Cs - Target		
	Calc.	Exp.	Ref	Calc.	Exp.	Ref
^{118}I	1.3	6	a)			
^{119}I	4.2	13	a)			
^{120}Xe	1.8	8.5	a)			
^{120}I	6.6	15	a)			
^{121}Cs	1.9	} 21	a)			
^{121}Xe	3.6					
^{121}I	14.8	18	a)			
^{122}Cs	4.6	} 42	a)			
^{122}Xe	12.3					
^{123}Ba	0.2	} 36±5	b)	--	} 4.21±0.94	e)
^{123}Cs	12.6	} 45±6	c)	49.4		
^{123}Xe	17.5	} 57±9	b)			
^{123}I	11.7	12	a)			
^{124}I	5.8	9.3	a)			
^{125}Ba	2.7	} 57±9	b)	--	} 95.8±13.5	e)
^{125}Cs	27.5	43	a)	53.5		
^{125}Xe	16.3					
^{125}I	3.4	6.7	a)			
^{126}I	1.3	5.1	a)			
^{127}La	2.4	} 45±7	b)	-	} 24.4±0.5	e)
^{127}Ba	18.7	} 29±8	c)			
^{127}Cs	11.9	59	d)	14.1		
^{127}Xe	5.1	} 53±11	b)			
^{128}I	0.2	1.3	a)			
^{129}La	21.2	} 68±14	b)			
^{129}Ba	22.3	} 51±8	c)		14.0±0.15	e)
^{129}Cs	3.0	35	d)	24.8	34.0±0.6	e)
^{130}Cs				34.3	55.3±6.4	e)
^{130}I	0.12	0.33	a)			
^{131}Cs				49.5	47.2±2.6	e)
^{131}I	0.05	0.15	a)			
^{132}Cs	11.7	6.1±1.8	c)	61.2	63.6±1.7	e)
^{136}Cs	0.32	0.86±0.03	c)			

Table 1b

Product	^{nat}Ba - Target			^{nat}Ce - Target			^{141}Pr - Target		
	Calc.	Exp.	Ref.	Calc.	Exp.	Ref.	Calc.	Exp.	Ref.
^{127}La	-			2.7			3.4		
^{127}Ba	20.1	21±5	c)	18.6	54±8	c)	20.3	49±8	c)
^{127}Cs	21.0			7.8			4.9		
^{129}La	-			20.0			22.9		
^{129}Ba	50.0	27±5	c)	39.2	66±9	c)	29.6	58±8	c)
^{129}Cs	23.4			1.7			0.96		
^{132}Cs	25.9	12±3	c)	1.0	2.8±0.6	c)	0.11	0.23±0.06	c)
^{136}Cs	21.8	7.7±2	c)	0.06	0.12±0.05	c)	0.005	0.011±0.008	c)

a) Ref. 2 b) ref. 3 c) Ref. 4 d) Ref. 5 e) Ref. 6

Tables 1a and 1b: Comparison between experimental and calculated cross sections. Units are mb. Calculations are done for 590 MeV proton energy and do not vary appreciably in an energy range of 40 MeV. Proton energies were 600 MeV for references b), 550 MeV for reference e) and 590 MeV otherwise

Table 2

Product	Target-nucleus													
	^{133}Cs	^{nat}Ba	^{139}La	^{nat}Ce	^{141}Pr	^{130}Ba	^{132}Ba	^{134}Ba	^{135}Ba	^{136}Ba	^{137}Ba	^{138}Ba	^{140}Ce	^{142}Ce
^{120}Xe	1.25	0.31	0.27	0.29	0.36	7.32	2.96	1.26	0.81	0.51	0.31	0.19	0.31	0.12
^{121}Xe	2.83	0.75	0.66	0.69	0.82	9.33	5.63	2.79	1.86	1.22	0.79	0.50	0.74	0.31
^{122}Xe	1.01	0.30	0.27	0.26	0.29	1.77	1.49	0.96	0.69	0.48	0.33	0.22	0.28	0.13
^{123}Xe	6.09	3.10	2.71	2.53	2.53	4.12	6.44	7.70	6.24	4.70	3.43	2.43	2.68	1.44
^{125}Xe	1.21	1.01	0.73	0.54	0.41	0.58	0.73	0.88	0.83	1.08	1.06	1.01	0.55	0.51
^{127}Xe	0.012	0.007	0.004	0.003	0.003	0.004	0.004	0.008	0.007	0.007	0.006	0.006	0.003	0.003
R	2.15	4.55	4.11	3.70	3.10	0.44	1.14	2.76	3.35	3.85	4.35	4.84	3.61	4.57

Table 2: Xenon activities produced by 4 hours of irradiation of different targets. Units are 10^{10} decays/sec. A proton flux of $2.4 \cdot 10^{13}$ / cm^2 sec of 500 MeV energy is taken. The targets consist of $5 \cdot 10^{22}$ atoms. Also shown is the ratio R = ^{123}Xe activity / ^{121}Xe activity.

References

{1} R. Silberberg and C. H. Tsao, Astrophys. J. Suppl. 25 (1973) 315, ibid. 25 (1973) 335

{2} R. Silberberg and C. H. Tsao, Cross Sections of Proton-Nucleus Interactions at High Energies, Naval Research Laboratory Report 7593, Washington 1973

{3} A. E. Ogard et al. in Accelerator-Produced Radioisotope Program, La-5249 PR, Los Alamos 1973

{4} K. L. Scholz et al., Int. J. Appl. Rad. and Isotopes 25 (1974) 302

{5} K. L. Scholz et al., Am. Assoc. Phys. in Medicine, Quarterly Bull., June 1972, p. 80

{6} M. A. Molecke in Nuclear Chemistry Research of High Energy Nuclear Reactions at Carnegie-Mellon University Annual Progress Report 1971-1972, Pittsburgh 1972

3. Yields of (μ^-,pxn) reactions

A. Wyttenbach, P. Baertschi, H. S. Pruys†, E. A. Hermes†

When a nucleus (with charge Z) captures a negative muon, the resulting compound nucleus deexites almost exclusively by emission of neutrons and γ-rays, giving products with charge Z-1. Emission of a proton, leading to products with charge Z-2, has a very low probability. Up to now this process was only known to occur in light nuclei (Z<20) with a few percent probability {1}; for medium nuclei an upper experimental limit of 1 to 3 percent was observed {2}.

The usual experimental technique of measuring de-excitation γ-rays in time-relation to the μ-stop is not useful do detect rare events such as (μ^-,pxn), because these are drowned by the signals from the much more abundant (μ^-,xn) reactions. We therefore had to resort to activation experiments. In these experiments it is possible to choose targets in such a way that the (μ^-,xn) reactions lead almost entirely to stable and/or to very short or very long-lived activities; it is thus possible to measure instable products of (μ^-,pxn) reactions practically free from interferences, what in turn gives the activation method the necessary sensitivity for these rare events.

The activities were performed at the SIN superconducting μ-channel. The number of muons stopped in the target were recorded by a conventional counter telescope. Targets with a thickness of 2 to 3 g/cm^2 were used. After activation, they were removed from the μ^--beam and measured on a Ge(Li) detector. γ-ray spectra were evaluated by an appropriate computer program {3}, and γ-ray intensities are used to calculate activities.

The results of these measurements, some of which still have a provisional character, are fiven in Table 1 and Figure 1. The errors given are standard deviations as obtained from one to four experiments for each target; they do not take into account systematic errors associated with the μ^--beam-monitoring or with the decay schemes used. (μ^-,pn) and (μ^-,p2n) reactions on a given nucleus have roughly the same probability. The probability of a (μ^-,p)

reaction is lower by a factor of 5. It can further be seen that the yields of all three reactions decrease approximately exponentially with the Coulombbarrier of the target nucleus. It is though that these results can be explained by a neutron evaporation mechanism. Indeed for a given target there is roughly a constant ratio between the yields for (μ,xn) reactions (as calculated for an evaporation mechanism and barring direct neutron emission {4} and the experimentally determined yields of the (μ,pxn) reactions.

Future work will supplement the experimental data, and the theoretical considerations will be refined.

References

{1} P. Singer, Springer Tracts in Modern Physics, 71, 39 (1974);
S. Charalamabus, Nucl. Phys. A166, 145 (1971)
{2} C. Petitjean et al., Nucl. Phys. A178, 193 (1971)
{3} P. A. Schubiger, J. Radioanal. Chem. 25, 141 (1975)
{4} J. Hadermann, private communication

† Physics Institute, University Zürich

Table 1

Yields of (μ^-,pxn) reactions (in units of 10^{-3}/stopped μ^-)

Target	(μ^-,p)	(μ^-,pn)	(μ^-,p2n)
^{55}Mn	2.0 ± 0.2	10.8 ± 0.7	8.7 ± 0.1
^{59}Co	1.8 ± 0.1	22.7 ± 0.6	9.8 ± 0.2
^{75}As	1.3 ± 0.1	6.9 ± 0.2	4.8 ± 0.2
^{94}Zr		4.3 ± 0.8	
^{133}Cs	0.46 ± 0.02	2.4 ± 0.3	1.8 ± 0.1
^{209}Bi	0.07 ± 0.03		

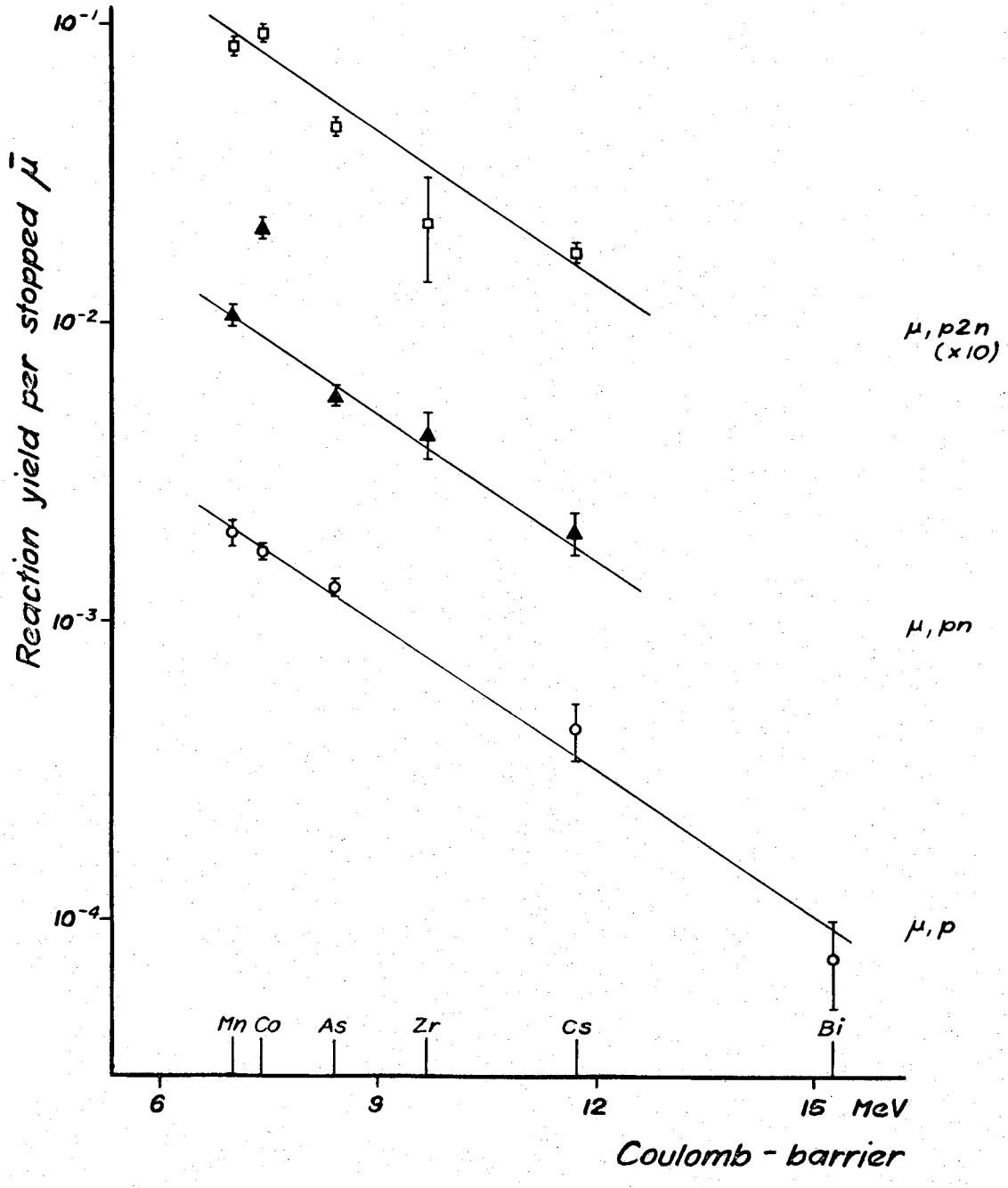

Fig. 1: Experimentally determined yields of (μ^-,pxn) reactions